nature biotechnology

FOCUS | REVIEW ARTICLE

https://doi.org/10.1038/s41587-019-0040-3

Accessing analytes in biofluids for peripheral biochemical monitoring

Jason Heikenfeld[1], Andrew Jajack[1*], Benjamin Feldman[2], Steve W. Granger[3], Supriya Gaitonde[3], Gavi Begtrup[4] and Benjamin A. Katchman[4]

Peripheral biochemical monitoring involves the use of wearable devices for minimally invasive or noninvasive measurement of analytes in biofluids such as interstitial fluid, saliva, tears and sweat. The goal in most cases is to obtain measurements that serve as surrogates for circulating analyte concentrations in blood. Key technological developments to date include continuous glucose monitors, which use an indwelling sensor needle to measure glucose in interstitial fluid, and device-integrated sweat stimulation for continuous access to analytes in sweat. Further development of continuous sensing technologies through new electrochemical sensing modalities will be a major focus of future research. While there has been much investment in wearable technologies to sense analytes, less effort has been directed to understanding the physiology of biofluid secretion. Elucidating the underlying biology is crucial for accelerating technological progress, as the biofluid itself often presents the greatest challenge in terms of sample volumes, secretion rates, filtration, active analyte channels, variable pH and salinity, analyte breakdown and other confounding factors.

It is impossible to imagine modern medicine without the ability to measure the presence, concentration or functional activity of analytes in biofluids, such as blood and urine. A first wave of technology development in the 20th century produced instruments for measuring nearly any desired analyte in these fluids, albeit with collection and transfer of the sample to a separate analytical laboratory (Fig. 1). The early 21st century witnessed widespread deployment of a second technological wave consisting of point-of-care diagnostics, which brought the laboratory into the hands of the doctor, nurse, first responder and patient. An emerging third wave now promises to allow patients to take the laboratory with them in the form of peripheral devices known as wearables[1]. For diabetes, all three of these technological waves are fully enabled; even wearable continuous glucose monitors now exceed $1 billion in market value[2]. However, commercially successful wearables remain elusive for chemical analytes beyond glucose. Finally, fully implantable biochemical sensing devices, which are already in development for glucose monitoring[3,4], can be considered the fourth technological wave in biofluid analyte measurement. These devices face steep technical challenges, and no such sensors that are reliable beyond hours or days of use exist for any analyte other than glucose. Thus, for the foreseeable future, peripheral biochemical monitoring will remain preferred over fully implantable devices.

In this review, we provide a critical analysis of peripheral biochemical monitoring with a focus on dermal interstitial fluid (ISF), saliva and sweat. Tears[5] are not discussed in detail here because they lack a compelling advantage over other biofluids (Table 1) and because access to tears is challenging both for one-time and for continuous measurements. We also discuss partitioning pathways—the pathways through which analytes are transported from blood into ISF, saliva and sweat. The analytes covered range from small ions and molecules to large proteins and antibodies (Table 2). Understanding partitioning pathways is essential to choosing the biofluids and analytes that might be most worthwhile to pursue and can help researchers avoid unfruitful, empirical-only studies of analyte correlations between blood and either saliva or sweat. Ultimately, technological advances in wearables are constrained by human biology itself.

Overview of biofluid sources

Analytes in blood are separated from ISF, saliva and sweat by thin, cell-based barriers. The morphology and composition of these barriers determine the ease and route of diffusion (Fig. 2). Below we discuss the barriers for analyte diffusion into ISF, saliva and sweat. (Partitioning into tears is similar to partitioning into saliva and sweat, but is not reviewed here; see "Conclusions and perspective" and Table 1).

Interstitial fluid. ISF is present in most of the dermis and also surrounds salivary and sweat glands (Fig. 2b,c,d). Therefore, understanding saliva and sweat requires knowledge of the relationship between capillary blood and ISF. Analytes in ISF come from blood, specifically through continuous capillaries. Considering that capillaries function to deliver nutrients, remove waste and exchange signaling molecules from blood with the surrounding tissues, they are leaky by design. There are three dominant ways that analytes enter ISF (Fig. 2a): first, diffusion through the plasma membrane of capillary endothelial cells (transcellular); second, diffusion and/or advective transport through the space between cells (paracellular); or third, vesicular transport through the cell (transcytosis). Small, uncharged analytes, such as steroid hormones like cortisol, readily diffuse through the plasma membrane. Most analytes of interest, such as charged analytes and proteins, cannot traverse this route and must be shuttled either through the endothelium via transport vesicles or through the paracellular pathway.

Continuous capillaries are made up of a single layer of endothelial cells joined by a flexible network of tight junctional strands that continuously break, reseal and branch (Fig. 2a,b). Ions (such as Na^+ or K^+) pass through these tight junctions. Small analytes (a few hundred daltons or less) can also pass through these tight junctions, but larger molecules rely on breaks in the tight junctions[6]. Periodic opening and closing of the compartments formed between tight junctions allows larger analytes to pass via the paracellular pathway. This general behavior for paracellular transport is common to ISF, saliva and sweat, but for ISF there is much less dilution of larger analytes. The capillaries feeding ISF have a diameter of only 5–10 μm. The high surface area-to-volume ratio, high capillary

[1]Novel Devices Laboratory, University of Cincinnati, Cincinnati, Ohio, USA. [2]Abbott Diabetes Care, Alameda, CA, USA. [3]Salimetrics LLC, Carlsbad, California, USA. [4]Eccrine Systems Inc, Cincinnati, Ohio, USA. *e-mail: jajackaj@mail.uc.edu

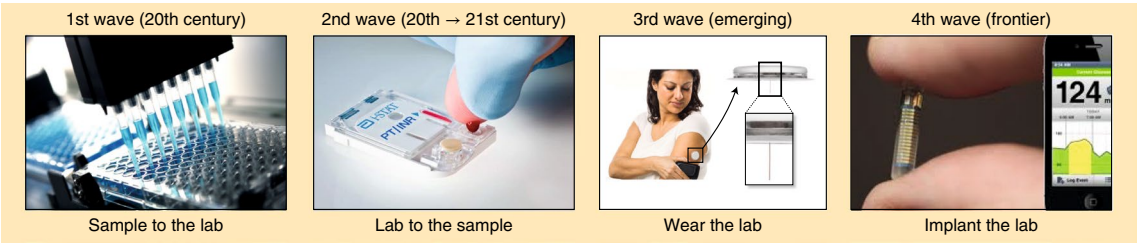


Fig. 1 | The four technological waves of biochemical monitoring.

Table 1 | Comparison of biofluids for peripheral biochemical monitoring

Biofluid	Molecular weight cutoff	Maximum dilution	Advective transport	Sample production	Lag time	Controllable secretion rate	Can require stimulation	Research maturity	Commercial maturity
ISF	~1 MDa	Up to 10×	Not needed	Tens of μL min^{-1} cm^{-2} [a]	~5–15 min	No, but steady	No	High	High
Saliva	Hundreds of daltons	>1,000×	Yes/no	Tens to hundreds of μL min^{-1} total	Tens of minutes	Difficult	No	High	Moderate
Sweat	Hundreds of daltons	>1,000×	Yes	0.1 to 2 μL min^{-1} cm^{-2}	Ones to tens of minutes	Yes	Yes	Medium	Low
Tears	Hundreds of daltons	>1,000×[78,79]	No	~1 μL min^{-1} (refs. [80,81])	-	Difficult	No	Low	None

[a]This is external extraction rate through suctioning, not necessarily the natural local production rate.

density, low flow rate, force produced by blood pressure, and ability of even large analytes (tens of kilodaltons) to enter via combined transcytotic and paracellular entry routes may contribute to the ease of fluid and analyte exchange between blood and ISF. As a result, many analytes have near equal concentrations between blood and ISF.

Saliva. Analytes in saliva originate primarily from capillaries that vascularize (feed) the salivary glands, which pass through ISF before entry. Salivary glands consist of end pieces, or acini, that specialize in producing a serous or mucous fluid (Fig. 2d). These acini are connected via narrow intercalated ducts. Saliva follows a path from acinus to intercalated duct to striated duct (intralobular) to excretory duct (interlobular), where it is drained into the oral cavity. The excretory duct has the largest luminal diameter, ~0.5–1.5 mm. Striated ducts have a diameter of ~60 μm, which is roughly three times that of the intercalated duct and approximately three to six times that of the acini[7,8]. The acini-linking intercalated and striated ducts are several millimeters in length, whereas the excretory duct can be several centimeters long[9]. The acini are the most vascularized portion because they have a higher metabolism, needed to support the energetics of saliva secretion. The secretory acini have a single-layer simple columnar epithelium, and the narrow intercalated ducts have a single-layer simple cuboidal epithelium and a high surface area-to-volume ratio. The paracellular partitioning route dominates for most analytes and results in substantial dilution of most analyte concentrations, but transcellular routes are also possible (see below).

Sweat. Sweat glands are generally similar to salivary glands, albeit much smaller in dimension and comprising a single tubule[10,11]. We focus exclusively on the eccrine sweat glands (involved in thermal regulation across most of the body surface) because apocrine sweat glands have the disadvantage of location in the axilla and groin, and they have a much more oily and bacteria-rich composition that can confound analyte measurement. Most of the gland is in the dermis, a largely acellular and porous collagen matrix filled with ISF (Fig. 2b,c). The sweat glands are highly vascularized in the secretory coil, which has a 5–40 μm inner diameter, a 2–5 mm length and an epithelium one to three cells thick. The dermal duct has a 10–20 μm inner diameter, a ~2 mm length and a two-layer stratified cuboidal epithelium. A 200–300 μm coiled duct spans the remaining epidermis and stratum corneum. Much as in salivary glands, the paracellular route of analyte entry also dominates, and, as in salivary glands, the paracellular route results in substantial dilution of most analytes (see below).

Below we provide a systematic review of each biofluid (ISF, saliva and sweat), focusing on the process of fluid creation or secretion, analyte partitioning into the fluid, and sampling and device technology, and ending with a discussion of the challenges and outlook for analyte sensing. Table 2 details the different types of analyte in each biofluid; these were chosen to represent analyte classes for which partitioning is heavily dependent on size (paracellular transport) and lipophilicity (transcellular transport). We provide a more in-depth discussion of glucose data throughout, as glucose is the most well-studied analyte in all three of these biofluids.

Interstitial fluid

ISF accounts for roughly three-quarters of extracellular fluid, with most of the other extracellular fluid being blood plasma. Sensing of glucose in ISF is now a mature field, but it is a singular achievement because robust approaches for ISF sensing of analytes other than glucose, even in a research context, are lacking.

Biofluid process. The blood plasma and ISF interact at the capillaries, which are permeable and allow water and small polar solutes to interchange freely between the two fluids by diffusion (Fig. 2a). In addition, the blood capillary hydrostatic pressure is higher than that of the ISF, and this encourages advective flow of solute-containing

Table 2 | Comparison of analytes representing several classes found in blood plasma, ISF, saliva and sweat

	Na^+	K^+	Lactate	Glucose	Cortisol	Drugs	Cytokines	Antibodies
Molecular weight (Da)	23	39	90	180	362	Mostly hundreds of daltons	More than five to tens of kilodaltons	Hundreds of kilodaltons
Lipophilicity	Very low (charged)	Very low (charged)	Very low (charged)	Low (hydroxyls)	High	Often high	Very low	Very low
Blood plasma	135–145 mM	3.5–5 mM	0.5–10 mM (resting to nonresting)	4.1–6.9 mM (venous, resting)	Hundreds of nanomolar total; tens of nanomolar unbound fraction	Mostly equivalent to unbound in plasma	Picomolar to nanomolar	Varies; total ~0.4–16 mg ml^{-1}
ISF[a]	Similar to plasma	Similar to plasma	Similar to plasma	Similar to plasma	Unbound similar to plasma (p)	Many equivalent to unbound in plasma (p)	80% of plasma (a,p)	15–25% of plasma
Saliva[a]	Tens of millimolar (a)[82]	Tens of millimolar (a)	Tenths to ones of millimolar[36,37]	~1% of plasma (p, fd)[76]	Unbound similar to plasma (p)	Many equivalent to unbound in plasma (p)	Local production dominates (a,p)	Local or very highly diluted (a,p)[83]
Sweat[a]	Tens of millimolar (a)[11]	~5–15 mM (under debate)[84]	~5–10's mM (a,p,fd)[85,86]	~1% of plasma (p,fd)[87]	Unbound similar to plasma (p)	Many equivalent to unbound in plasma (p)	<0.1% of plasma (mainly p, some a)[68]	Local or very highly diluted (a,p)[62,88]

[a]For ISF, saliva and sweat, (a) indicates active channel or actively locally generated, (p) indicates passive partitioning into the fluid, and (fd) indicates possible high dependency on flow rate.

water from the plasma to ISF. The paracellular pathways (Fig. 2a) in the capillaries are sized such that they offer little restriction to small polar solutes, but do exhibit a filtering effect on larger macromolecules (proteins and lipids). Furthermore, as the lymphatic system continually removes ISF, fluid pressure is negative relative to atmospheric pressure, by about 500–1,000 N m^{-1} (refs. [2,12]). This negative pressure complicates sample extraction. In addition, in the dermis, where ISF is analyzed with wearable devices, the capillary density is low because the dermis is largely acellular and because the epidermis is metabolically slow. Therefore the exchange process between plasma and ISF in the dermis results in some delay between rapidly changing plasma concentrations and their concentrations in ISF, even for small polar solutes. This phenomenon is called ISF lag and is especially important in ISF glucose monitoring.

Equilibrium analyte partitioning. For many analytes, a fairly simple relationship exists between equilibrium ISF and plasma concentrations. The discussion here for ISF, as well as for saliva and sweat below, will follow the analytes listed in Table 2. For low molecular weight species (for example, Na^+, K^+, glucose (Fig. 3a) and lactate), the ISF concentration is very similar to the plasma concentration. This similarity in concentrations benefits from the fact that paracellular diffusion through the capillary walls is rapid compared to the turnover rate for ISF from the dermis. For example, a study of 20 subjects found an average [Na^+] of 141.2 mM in plasma and 135.7 mM in ISF. Similarly, [K^+] was found to be 4.37 mM in plasma and 3.97 mM in ISF[13]. Likewise, for glucose at equilibrium, a large body of commercial sensor data indicates that the plasma and ISF concentrations are nearly identical. Fewer data exist for ISF lactate, but lactate's smaller size and much higher diffusivity (compared with glucose) suggests a near unity plasma/ISF ratio. For cortisol (362 Da), the situation is more complicated. For example, cortisol has a total plasma concentration ranging from 80–500 nM (with a clear diurnal variation), but has been found in the ISF at a loosely correlated and much lower concentration of 5–50 nM[14]. This is likely because in blood, assays often measure total cortisol, and most cortisol in blood is bound to proteins. These proteins, such as transcortin, are diluted in ISF. However, free cortisol is highly lipophilic and can therefore transition transcellularly through the capillary lining, resulting in similar concentrations of unbound cortisol in blood and ISF. The unbound cortisol is also the active fraction and is, therefore, a useful measurement in itself.

For drugs such as penicillin and diamorphine, the relationship between plasma and ISF concentrations is complicated by their short half-life. This means their concentrations change rapidly after administration and might not reach steady state values. For example, with penicillin G in sheep, administration of 53 mg/kg resulted in a plasma/ISF concentration ratio of about 9 after 10 min, decreasing to almost unity after 2 h[15]. Also, like cortisol, a portion of penicillin in plasma is protein bound[16]. Diamorphine is more lipophilic than penicillin, so, like cortisol, it should readily partition into ISF without filtration. However, diamorphine is even more fleeting and cannot even be detected in rat blood 18 min after administration because it is rapidly metabolized[17]. Other small lipophilic drugs with longer metabolic half-lives (on the order of hours) are more likely to yield useful correlations with blood concentrations.

For higher molecular weight species, such as proteins and lipids, the ISF/plasma concentration ratio has been found to vary in an inverse logarithmic relationship with molecular weight[18]. Therefore, a conversion factor may be required for interpretation of diluted analyte concentrations in ISF. This trend is unsurprising, given the filtering effect of blood-to-ISF paracellular transport through tight junctions (Fig. 2a). ISF/plasma concentration ratios for proteins vary from 0.9 for insulin (6,600 Da) to 0.29 for albumin (68,500 Da) to 0.14 for α-2 macroglobulin (775,500 Da). These partition coefficients vary directly with diffusion coefficient, which is dependent on molecular weight and ranges from 2×10^{-7} to 15×10^{-7} cm^2 s^{-1} for the above three proteins. Lipids follow a similar relationship, with high-density lipoprotein (~250,000 Da) and low-density lipoprotein (~750,000 Da) present in ISF at ~25% and 20%, respectively, of their plasma concentrations. Antibodies are also very large and therefore likely to have a similar molecular weight dependence.

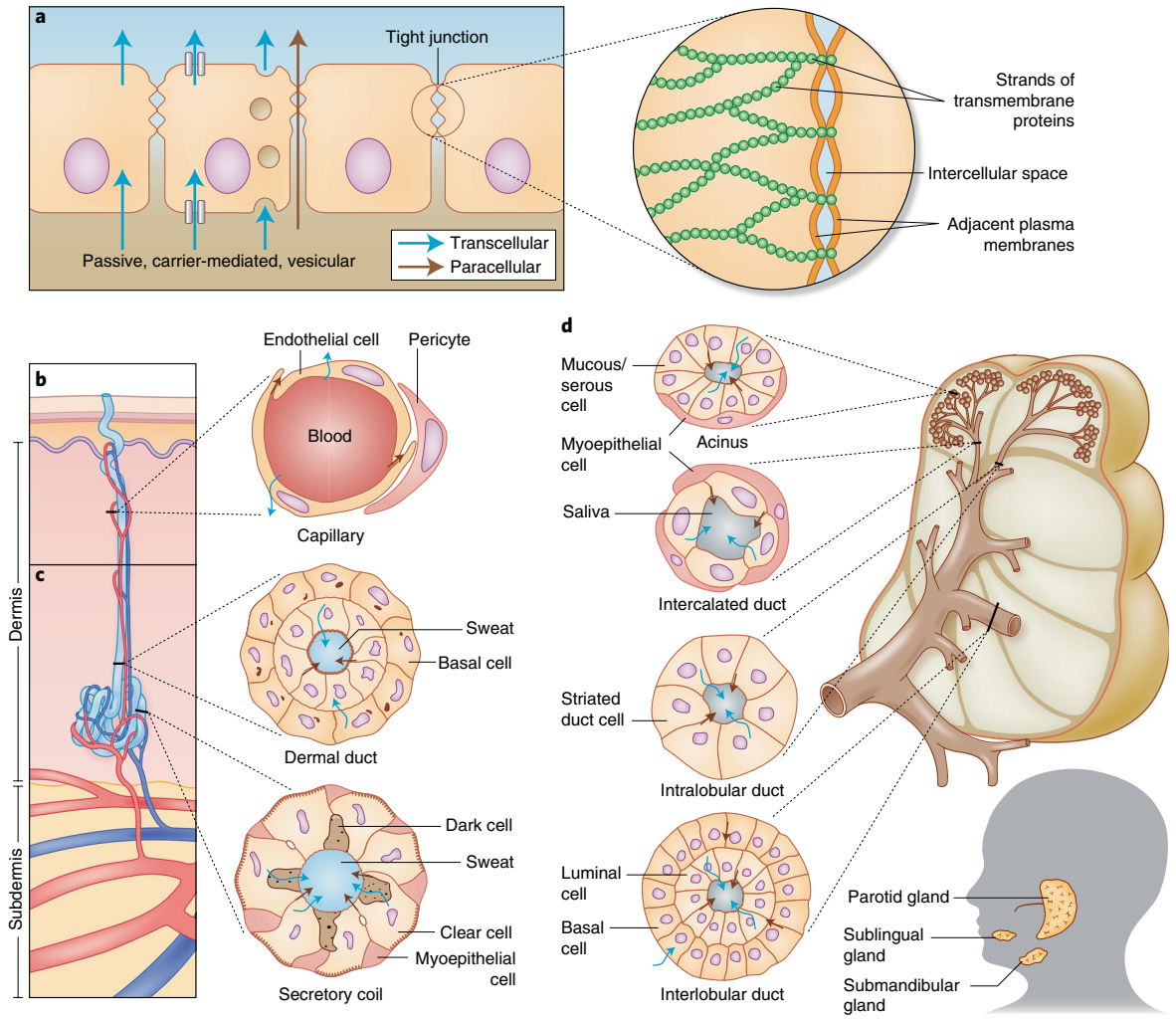


Fig. 2 | Characteristics of the glands and biofluids discussed in this Review. a, Biomarkers enter ISF, sweat and saliva via either transcellular or paracellular routes. Tight junctions (right[74]) form the paracellular barrier but undergo constant remodeling that allows larger solutes to pass. The structure and surface-area-to-volume ratio of the cellular barriers determine the ease and route of entry of analytes into each biofluid. **b**, In ISF a net fluid flow from blood is driven by hydrostatic pressure. Even larger analytes (1's to 10's kilodaltons) are found at concentrations similar to those in blood. **c**,**d**, In sweat (**c**) and saliva (**d**), a net fluid flow is driven from blood and ISF by osmotic pressure, and the cellular barriers to analyte transport are greater, such that most analytes are diluted compared to blood, with the exception of transcellular transport by carrier mediation or by passive diffusion of small lipophilic analytes.

Dynamic analyte partitioning. When solute concentrations change rapidly in the plasma, there is a time delay before the corresponding change appears in the ISF. This ISF lag is particularly significant in glucose monitoring. For ISF glucose sensors, which are typically indwelling electrochemical sensors (placed through the dermis into the subcutaneous fat using a metal needle), this lag is the sum of the inherent device response time (typically 1–5 min as glucose diffuses through the sensor's flux-limiting membrane) plus the inherent plasma-to-ISF lag (typically estimated at 5–10 min, with some subject-to-subject variability), leading to a total raw ISF device lag for indwelling electrochemical glucose sensors of 5–15 min.

However, in continuous sensors, this device lag can be cleverly minimized by data processing algorithms that use the preceding data stream to accelerate the sensor's reported response to changes in ISF glucose. For example, the actual reported ISF lag for the FreeStyle Libre Flash Glucose Monitoring System (Fig. 3a,c), an indwelling ISF glucose sensor, was 4.5–4.8 min[19]. The ISF lag for larger molecules and proteins is not well studied and is likely to be slower if considerable diffusion to the sensors is needed. But many of these larger analytes change slowly in concentration in blood as well, and sensing could therefore effectively be 'real time'. For microneedles (Fig. 3b,d,e), the sensors typically dwell outside the body and glucose must diffuse to the sensor through a microneedle that is hundreds of micrometers long, creating a total unaccelerated lag time of approximately 17 min (Fig. 3b)[20].

Sampling technology and devices. ISF can be measured either by withdrawing the sample from the body and testing externally or by using an indwelling sensor that resides in the tissue and is bathed in ISF (Fig. 3c)[21]. Examples of sample withdrawal techniques include microdialysis (used by the Glucoday CGM from Menarini) and reverse iontophoresis (formerly used in the GlucoWatch CGM from Cygnus). Reverse iontophoresis involves driving a flow of positive ions outward through the skin by an electric field (voltage). In skin, reverse iontophoresis further creates paracellular electro-osmosis (advective fluid flow) because the negatively charged plasma membranes attract a moving electro-osmotic sheath of positive ions (Na^+, K^+, etc.). With the GlucoWatch, a current density of ~0.5 mA cm^{-2} extracted ISF at rate of ~5 to 50 nL min^{-1} cm^{-2}. Because the pathway for electro-osmotic flow is paracellular, the resulting fluid is a filtered form of ISF and not pure ISF, somewhat similar to sweat or saliva. Microdialysis requires the insertion of a small microdialysis

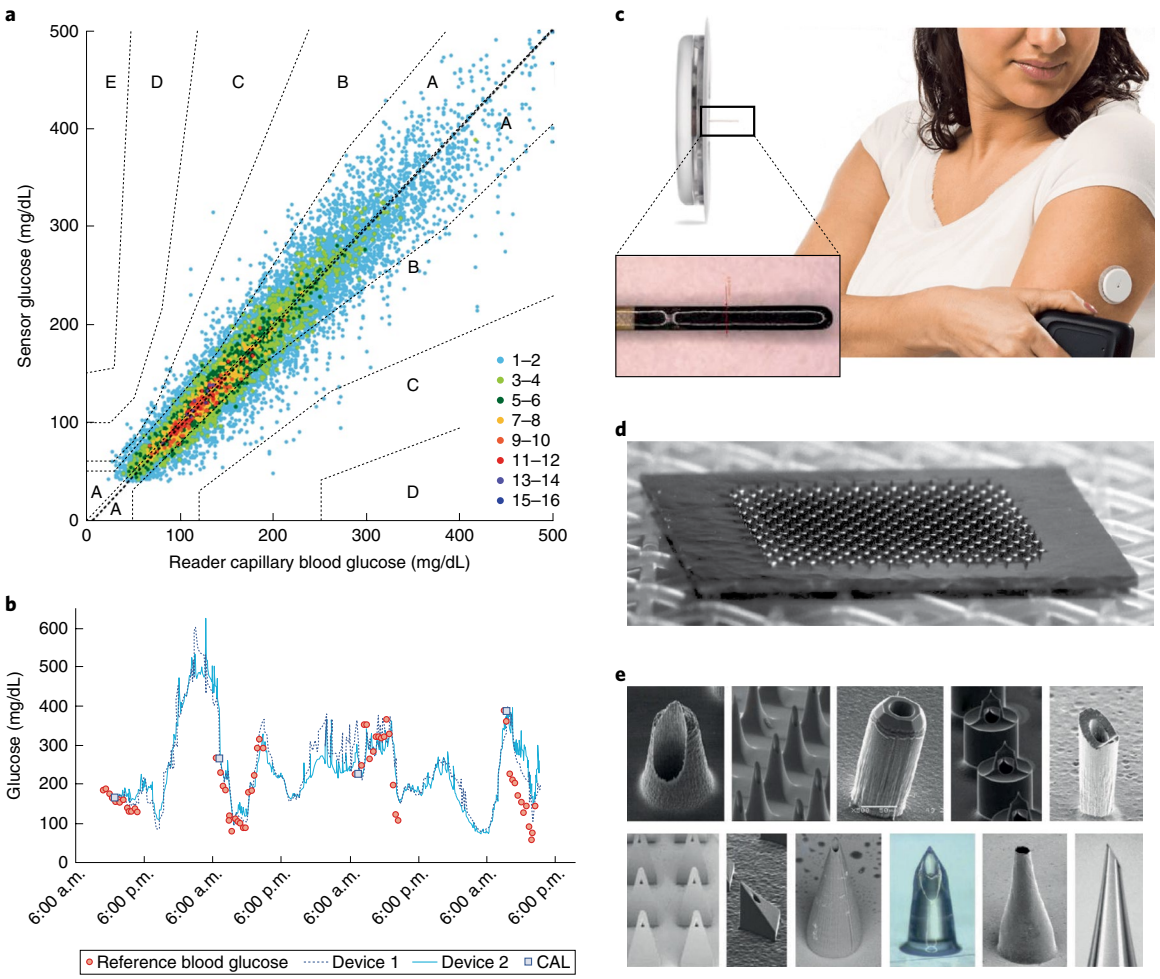


Fig. 3 | Correlation between blood glucose and ISF glucose measured on different devices. a, Consensus error grids analysis of data from a FreeStyle Libre Flash Glucose Monitoring System, in which a needle-like glucose sensor is inserted into the dermis[19]. Colors correspond to the number of overlapping data points. **b**, Data from an Arkal Medical microneedle device, which uses sensors outside the body; this system has a longer total lag time than the device in **a** because glucose must diffuse through the microneedles to the sensor[20]. Two devices (Devices 1 and 2) were worn simultaneously by a subject to demonstrate interdevice precision. Devices were calibrated (CAL; designated with a square symbol) using a reference blood glucose value after an initial 2-h warm-up period and then once daily. **c**, Abbott FreeStyle Libre Flash Glucose Monitoring System, used to collect the data shown in **b**. **d**, Arkal Medical microneedle device, used to collect the data in **b**[20]. (**e**) Different types of inorganic and polymer microneedles[75].

catheter into the skin, with a semipermeable membrane that allows small analytes (molecules, ions) to exchange with a fluid in the probe. This fluid can then be extracted and sensed.

Unfortunately, in general, sample withdrawal of ISF has several drawbacks, including the cumbersome size of the mechanical hardware (for example, vacuum) and thus of the device required for sample withdrawal; the time required for sample withdrawal, which directly increases the ISF lag; in the case of iontophoresis (which requires no mechanical hardware), the need to apply voltages, which can cause skin irritation over the long term; and the onset of sweating, which can confound the measurement accuracy. Furthermore, it is not certain whether ISF samples can be reliably extracted through needles or poration of the skin without altering analyte concentrations[22]. For example, analyte concentrations can be altered by dermal compaction by the wearable device and/or by strong suctioning, which changes the pressure balance between blood capillaries, ISF and lymphatic capillaries.

Indwelling electrochemical ISF sensors are much simpler in concept than those that require withdrawing ISF and have, in the case of glucose, gained widespread and growing market acceptance. For example, in the FreeStyle Libre Flash Glucose Monitoring System from Abbott Diabetes Care (Fig. 3c), the spring-loaded inserter is first mated with the sensor pack containing the sensor and insertion sharp. This is then applied to the skin, leaving the on-body electronics adhesively attached to the skin, and electrically connected to the transdermal sensor, which is bathed by ISF ~5 mm below the skin surface. The insertion sharp is a slotted needle with a cross-sectional area of 0.29 mm^2 and a length of 8.5 mm. Glucose readings are obtained by swiping the on-body electronics with a near-field communication–enabled meter or phone. This system measures and records glucose data for 2 weeks for each deployed sensor and does not require external calibration with a reference blood glucose device. An example of data obtained by this device is shown in Fig. 3a. In a study[19] in which 72 participants wore the ISF sensor for a 2-week period and sensor results were compared with eight blood glucose test strip reference measurements per day, for a total of 13,195 paired points, 86.7% resided in the clinically accurate consensus error grid zone A, meaning that 86.7% of readings would have caused users to take exactly the appropriate action regarding insulin or food intake.

An alternative approach, either to full sample withdrawal (microdialysis and reverse iontophoresis) or to full sensor immersion (implanted electrochemical sensors), is microneedle arrays (Fig. 3b,d,e), which breach the skin and create a short fluid path

(~500 μm) for analytes to diffuse from the ISF to an adjacent ex vivo sensor. In this way, fairly accurate (mean absolute relative difference = ~15%, compared with ~10% for the best available commercial devices) continuous glucose data have been obtained from limited patient numbers for up to 72 h[20]. This approach is attractive because it is minimally invasive, but it faces an uphill battle to meet the robustness and accuracy of existing indwelling sensors. In addition, because of the multiple breaches through the skin due to a large array of needles, swelling and irritation can occur, which could lead to noncompliance or product rejection[23].

Challenges and outlook. Continuous ISF glucose measurement is widely accepted and rapidly growing. For example, in January 2018, it was estimated that 31% of people with type 1 diabetes use ISF glucose sensors, and that number was projected to increase to 44% by 2020. Similarly, for insulin users with type 2 diabetes, ISF monitoring was projected to expand from 17% to 26% of the total population over the same period[24]. This has been driven largely by ongoing improvements in accuracy, convenience and cost. Clearly, for glucose monitoring, ISF is supplanting blood as the fluid of choice.

Expansion to non-glucose ISF measurements is an area of active interest and will, to a great extent, depend on developing linear and stable sensors that replicate the accuracy and stability of commercial glucose sensors, which took many decades to optimize. Each time a new sensor is applied, the skin barrier must be breached, resulting in minor scarring and a low but real risk for infection. As a result, sensor stability (lifetime) is a particular concern and chief hurdle for other analytes because shorter sensor lifetimes require more skin-breaching events. The issue of stability is further complicated by the advent and wide commercial acceptance of factory-calibrated sensors, which further elevate the bar for acceptable stability, considering that factory-calibrated sensors must maintain an unchanging sensitivity during 1–2 years of shelf storage, a requirement dictated by the logistics of sensor production and distribution[25]. Furthermore, many other analytes of interest occur in much lower (micromolar to picomolar) concentrations, and for these analytes, not only must stability concerns be addressed, but also new, nonamperometric techniques must be developed. Only one class of sensors based on electrochemical aptamers[26] has been proven for micromolar to nanomolar detection in blood and plasma, and therefore shows initial potential for detection in ISF.

Saliva

Saliva is a dilute (99% water), heterogenous secretion into the oral cavity. Sensing technologies in saliva are not frequently the focus in the field of salivary diagnostics. The lower necessity for sensing technologies in saliva is due in part to the relative ease of collecting adequate quantities of saliva for more conventional tests. However, in circumstances that require immediate feedback about the test subject or patient (point of care), sensing in saliva is crucial.

Biofluid process. Each class of molecules enters into saliva by active or passive means on the basis of its size, hydrophilicity and charge. Although most of the secretion volume and electrolytes in saliva originate from the three major salivary glands (the parotid, submandibular and sublingual glands), minor glands contribute less volume but more of the blood plasma components. Saliva generation in each gland type is somewhat different, but all share a common ion secretion process, which causes an osmotically generated water influx. Saliva also mixes with gingival crevicular fluid, a serum-like exudate that carries several key components of the immune response (molecular complement components and antibodies, cellular neutrophils and plasma cells). Gingival crevicular fluid acts as a defense barrier to tissue invasion by subgingival plaque bacteria.

The relative contributions of each salivary gland during unstimulated flow are 20% from parotid, 65% from submandibular, 7% to 8% from sublingual, and less than 10% from numerous minor glands[27]. Salivary composition and secretion are dependent on the type of gland, time of day, age, gender and stimulus[28]. Saliva production originates in the acinar cells of the salivary gland (Fig. 2d), and salivary secretions are defined as serous, mucous or mixed; serous secretions are produced mainly from the parotid gland, mucous secretions from the minor glands, and mixed serous and mucous secretions from the sublingual and submandibular glands[27]. During production, fluid travels from the acini through the ducts to the oral cavity. As substances enter saliva from the vascular system, they travel through multiple barriers, including the capillary wall, the interstitial space and the cellular lining of the gland. The rate of salivary flow is highest in the morning and slows through the course of the day, with almost no saliva production at night[29]. A normal average daily rate of saliva production can be as much as 1.5 liters or as little as 500 ml per day, of which ~90% is considered stimulated (typically by taste or smell) as defined by a flow rate above 0.2 ml per minute. Unstimulated saliva is often referred to as passive drool and defined by flow rates between 0.1 and 0.2 ml per minute.

Unstimulated and stimulated saliva differ in the concentration and composition of oral fluid components. These differences are mainly attributed to different contributions made by the salivary glands. For stimulated saliva, secretion can be evoked by different means, each of which can induce different salivary glands to contribute specific contents[30]. Saliva secretion is regulated by parasympathetic and sympathetic neural pathways. Sympathetic nervous system stimulation in rats yields saliva with increased protein concentration, whereas parasympathetic nervous system stimulation leads to a more watery saliva[30]. Stimulated saliva creates a diagnostic challenge for measuring analytes that are charged or larger in size because their concentrations become more dilute as salivary flow rates increase. Therefore, flow-rate measurement may be required to normalize some analyte measures. Most diagnostic procedures rely on unstimulated saliva samples. A considerable challenge for the design and placement of a wearable device lies in the fact that saliva varies in composition in different regions of the mouth[31].

Analyte partitioning. The partitioning of analytes in saliva[32] will be illustrated in this section by a description of the behavior of each molecule listed in Table 2. The saliva generation process is dependent on chloride secretion by the acinar cells, which causes an electrical potential to form across the cellular lining of the salivary gland. This potential then draws in positively charged ions such as Na^+ through a paracellular pathway (through the tight junctions; Fig. 2a), which generates an osmotic gradient that brings water through apical aquaporin channels into the ducts. The ductal portions of the gland then reabsorb much of the Na^+ and Cl^-. Although saliva may seem an attractive sample for measuring electrolytes or osmolality to determine bodily hydration status, the variability of salivary data and the influence of confounding factors have limited its utility[33] for this purpose.

Salivary glucose represents a small hydrophilic molecule that enters saliva through the paracellular route and also moves easily from blood plasma to the gingival fluid through the gingival sulcus[34]. Some studies indicate that glucose in saliva correlates well with blood plasma levels (Fig. 4a); however, this association requires a fasting sample (no food or drink contamination), which minimizes its utility for patients with diabetes. Other researchers have reported less favorable correlations[35], but despite this controversy there remains interest in salivary glucose[24].

Lactate is another analyte that represents hydrophilic molecules that enter by the paracellular route but also to some extent from gland metabolism, which can make blood correlation difficult. A good correlation for lactate has been reported ($r = 0.81$) between saliva and capillary blood obtained by finger prick when samples are taken during exercise[36], and other promising results have been reported[37].

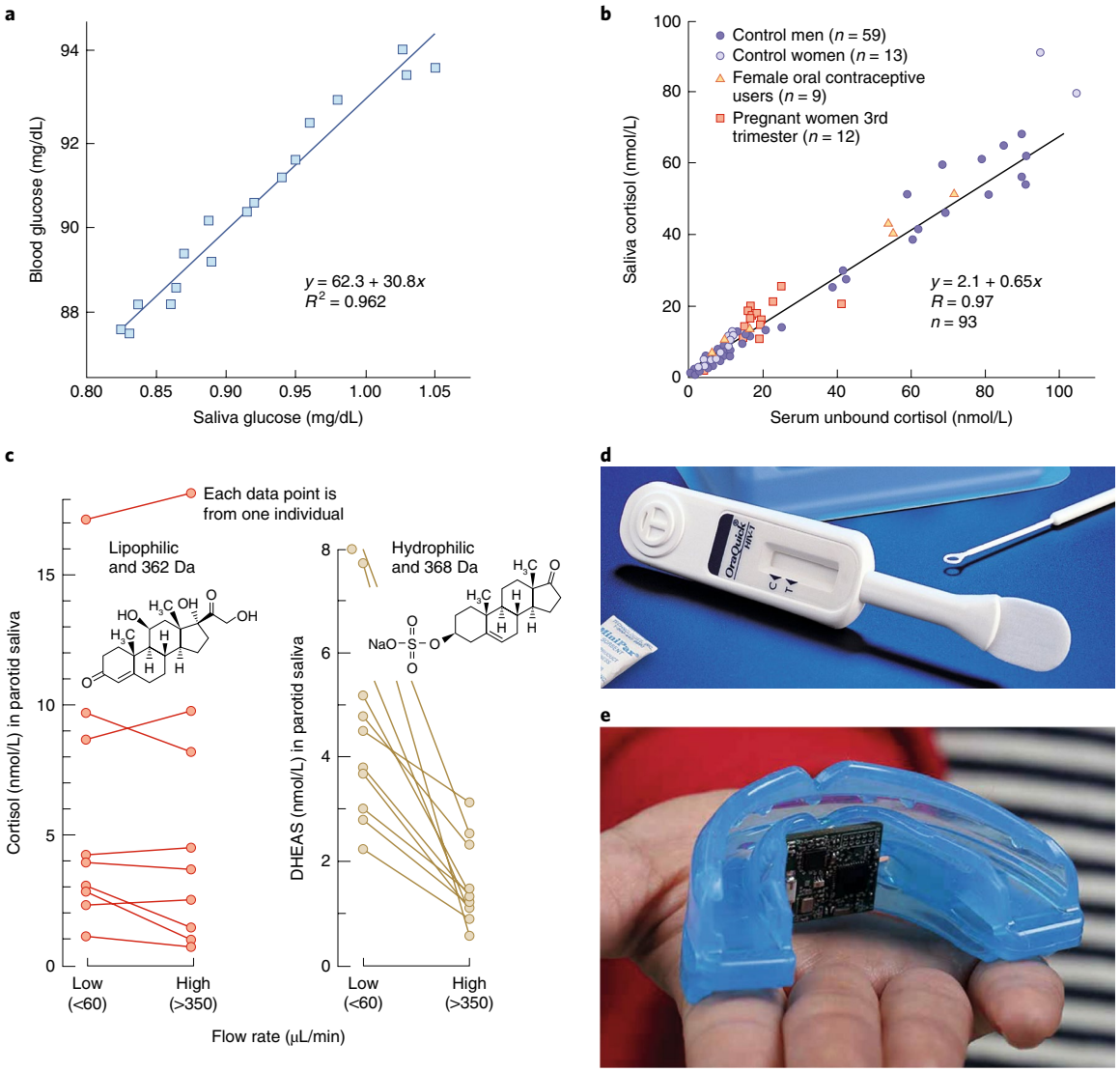


Fig. 4 | Correlation between different bioanalytes in the blood and saliva and examples of different devices for analyzing saliva. a, Glucose blood correlation with saliva[76]. **b**, Cortisol blood correlation with saliva[77]. **c**, Dilution data for cortisol and dehydroepiandrosterone sulfate (DHEAS), which are two similarly sized analytes but with very different lipophilicity[39,51]. **d**, Simple use-at-home salivary tests for HIV status. **e**, Emerging technology for mouth-wearable electrochemical saliva sensing of uric acid[49].

Lipophilic molecules such as hormones enter saliva from the blood plasma by passive diffusion through the lipophilic layers of the capillaries and glandular epithelial cells and therefore correlate well with unbound fractions in blood plasma. Accordingly, lipophilic drugs can also easily enter saliva, which could serve as a useful biofluid for drug monitoring[38]. However, some unbound charged steroid hormones are influenced by flow rate, and samples obtained for these measurements should avoid stimulated flow, which could affect these correlations (Fig. 4b,c)[39].

Some cytokines and proteins are produced by cells in the salivary glands or by immune cells present in the oral cavity. As a result, these analytes typically do not correlate well with plasma concentrations because they are locally produced. However, levels of inflammatory cytokines that are locally produced do reflect the oral health status (not body health) of the subject. In fact, levels of IL-1β, TNF-α, IL-6 and matrix metalloproteinases have been associated with gingivitis and periodontal disease and have diagnostic value[40–42]. One exception is C-reactive protein (CRP), which is synthesized and secreted from the liver and hence reflects systemic inflammation; its salivary concentration correlates very well to plasma levels[43]. As with ISF, there is a substantial lag in appearance of peptides and proteins that are not actively transported in saliva after they appear in the serum. For instance, with insulin, the lag time is ~30 min, which limits the utility of point-of-care analysis for measures of this nature unless the lag time is incorporated into the measurement[44]. This lag time, like that observed for cortisol, is due to the time it takes for analytes to partition in ISF surrounding the salivary glands and/or leak into the gingival crevicular fluid from the capillaries, and then into saliva and fill the significant volume of the oral cavity.

Antibodies in saliva, mostly secretory IgA and to a lesser extent IgG, are thought to serve in a protective mucosal immune role against invading pathogens. Secretory IgA levels, produced by local plasma cells that reside in the stroma of salivary glands, are at higher levels than in blood and typically do not correlate well with plasma concentrations as they are produced in the oral cavity. However, their measurements are relevant within the context of mucosal humoral immunity. Secretory IgA enters saliva by active transport, whereas IgG is thought to enter by passive leakage via gingival crevicular fluid. Levels of salivary pathogen-specific antibodies are lower than in blood but high enough to determine

pathogen exposure in laboratory tests and point-of-care methodologies (for example, diagnostics for HIV[45–47]). Much as for ISF, a conversion factor may be required for interpretation of diluted analyte concentrations in saliva.

Sampling technology and devices. In the first wave of salivary diagnostics that began in the late 1970s, samples were collected and sent to central laboratories, where analytes were measured primarily by immunoassays or mass spectroscopy. For the most part, this type of approach remains in high demand in the research field, where large cohorts are studied, often over time, and samples are banked for testing at the end of the study in centralized testing laboratories. Routine instructions for sample collection include no food 30–60 min before collection, a water rinse of the mouth 10 min before to assure no interfering food particles, and at least a 30 min wait period after tooth brushing to avoid blood contamination[48]. For non–point-of-care applications, whole saliva samples are often collected as passive drool directly into a collection device or with swab material of varying compositions.

For the second wave of technology beginning in the 1990s, point-of-care tests have come of age and are used when on site-testing and diagnosis are essential. Lateral flow assays have become attractive for infectious disease detection, such as for HIV (Fig. 4d). However, for more quantitative detection, lateral flow assays have been challenged by difficulties posed by flow issues due to the heterogeneity in viscosity of saliva and the often unpredictable nature of dilution in saliva.

Wearable devices that represent the third wave of diagnostic technology have exploited devices, such as mouth guards equipped with electrochemical sensors, that sample saliva and detect molecules like uric acid in real time (Fig. 4e)[49]. Other wearable microsensors have been developed; however, none has yet established a lasting presence on the market. Another recently reported real-time salivary diagnostic method that may be considered a wearable uses the taste buds of the patient as a sensor to detect enzymatic activity associated with increased risk of peri-implant disease. In this case, a tasteless substrate in a chewing gum is used and produces a bitter product if cleaved because matrix metalloproteases are present[50]. One of the most popular uses for saliva to date is for isolation of genomic DNA for ancestry or other genotyping services. The devices for DNA isolation are varied, but consist of a collection cup, preservative and tube that can be sealed for shipping in the mail.

Challenges and outlook. Challenges to salivary diagnostics include sample heterogeneity, a usual necessity for pretreatment before testing, normalization for flow rate for quantitative assays, and proper sample handling after collection. Easy sample access enables at-home collection, with appropriate instructions ahead of sample collection mitigating the risk of samples being mistreated or lack of compliance in sample collection. For study of circadian biology that requires frequent sampling throughout the day (cortisol, melatonin, etc.), blood is inconvenient. Furthermore, sex hormone panels help diagnose maladies associated with menopause and timing of egg harvests for in vitro fertilization.

The US Food and Drug Administration has approved an over-the-counter at-home HIV test called OraQuick. OraQuick uses a lateral flow assay with a diagnostic specificity of 99.98% and sensitivity of 93% (Fig. 4d). As mentioned previously, saliva also has value in assessing oral health (gingivitis, periodontitis, cancer, etc.). Saliva will likely continue to play a valuable role for the first and second waves of diagnostics (sample to the lab or point-of-care use). However, as noted previously, for the third wave of wearable or continuous biosensing, these devices will need to resolve the challenges associated with saliva heterogeneity, variation between sampling sites, and changing sampling volumes between a device and the glands, and when relevant, those presented by increasing competition from ISF and sweat biosensing.

Sweat

Although eccrine sweat gland secretion has similarities to saliva and tears, substantial differences exist. Eccrine sweat biosensing has been an underdeveloped area of research and development, likely because only recently has it been realized that it can be a meaningful source of some analytes[51] and because only recently has integrated sweat stimulation been demonstrated to ensure prolonged, continuous access to sweat[52,53]. The only major application thus far is for one-time (point-of-care) cystic fibrosis testing by checking for elevated sweat chloride[54].

Biofluid process. A sophisticated stimulation pathway mediates the secretion of sweat, starting with acetylcholine activation of both muscarinic and nicotinic receptors in the myoepithelial cells lining the secretory coil and resulting in active secretion of chloride[55]. As in our description of ISF and saliva, our discussion here focuses primarily on aspects of secretion that influence analyte partitioning. Chloride secretion causes an electrical potential to form across the cellular lining of the secretory coil, which then draws in positively charged ions, predominantly Na^+, paracellularly (Fig. 2a). Because transmembrane proteins provide cell membranes with a net negative potential, the Na^+ ions travel as a sheath of ions close to the cell membranes, causing electro-osmosis and therefore a net advective flow of fluid into the secretory lumen[56]. The increased Na^+ and Cl^- in the secretory lumen also creates a negative osmotic pressure compared with ISF, resulting in an even more substantial influx of water, both transcelluarly through aquaporins[57] and through paracellular flow.

This sweat secretion process occurs in a pulsatile manner. The sweat generation rate varies from 0.1 nL min^{-1} per gland to >10 nL min^{-1} per gland, and, using a simple volume-filling argument, at high sweat generation rates a 5 nL gland replenishes its volume as fast as every few minutes[11]. Furthermore, because the secretory coil of the sweat gland is highly vascularized, the lag time in sweat can be quite rapid, even within 2–5 min of circulating blood changes[58]. Recently, it has been shown that wearable sweat ethanol sensors can initially detect an oral ingestion of ethanol within several minutes[59]. However, beyond ethanol, lag time data for sweat is lacking, and lag time for proper correlation with blood plasma might be longer and track more closely with lag times for ISF. Sweat generation is capable of generating pressures up to ~70,000 N m^{-2} (ref. [11]), which is enough pressure P for sweat (surface tension $\gamma \approx 70$ mN m^{-1}) to penetrate a hydrophobic pore with a radius r of 2 μm according to $P=2\gamma/r$. Sweat generation is therefore clearly more than adequate for pushing the sweat into a microfluidic or sampling device[60] (tens to hundreds of micrometers). Eccrine sweat gland densities range from tens to hundreds of glands per square centimeter depending on body location[11], and the resulting total sweat generation rate can therefore vary from 1 nL min^{-1} cm^{-2} to thousands.

Analyte partitioning. Partitioning for sweat is best shown by the same illustrative examples that were used for ISF and saliva (Table 2). Na^+ and Cl^- secretion, as discussed above, is dominated by the sweat secretion process, has no correlation with blood Na^+ levels, and increases from ~10 mM to ~100 mM with increasing sweat generation rate[11]. A useful evolutionary feature of the ductal portion of the sweat gland is the recapture of Na^+ and Cl^- to prevent excessive electrolyte loss. At higher sweat rates, there is simply less time to recapture Na^+ and Cl^-, and thus their concentrations increase. For K^+, some studies suggest that sweat K^+ is independent of sweat generation rate and that it may fall within blood plasma concentrations[61]. Whether or not K^+ correlates with blood plasma remains to be demonstrated. A meaningful sweat–plasma correlation for K^+ may ultimately be difficult to establish because changes in K^+ in blood plasma are very small and contamination and other confounding issues may dominate sweat K^+ levels.

Sweat glucose is a particularly illustrative example of the partitioning pathway and of the effects of sweat generation rate and dilution on analyte concentration. The speculated entry route for sweat glucose is paracellular. The paracellular route, while dimensionally large (>10 nm between cells[62]), is highly filtered by tight junctions of >40 different proteins. Of these proteins, the claudin family (Fig. 2a) has emerged as the most critical for defining tight junction selectivity. Tight junctions in sweat glands, much as in saliva, filter and dilute many larger analytes[62], necessitating a conversion factor for correlating with blood concentrations. As a result, sweat glucose is only ~1% of the glucose concentration in the surrounding ISF[63]. Also much as in saliva, this filtering (dilution) mechanism results in a likely concentration dependence on sweat generation rate[56].

A sweat glucose study[63] using short-lasting (<90 min) pilocarpine-stimulated sweat found that this stimulation results in variable sweat rates, yet some sweat-blood correlation is observable (Fig. 5a). Long-lasting (>6 h) sweat stimulation with carbachol[52], collected over a day as sweat rate slowly decreases, demonstrated a clear dependence of glucose concentration on sweat generation rate[56] (Fig. 5b). Further evidence of filtering is shown in Fig. 5c, whereby using chelation (citrate) for opening the tight junctions between the cells lining the sweat gland (Fig. 2b,c) results in an increase in glucose flux into sweat with application of reverse iontophoresis (electro-osmosis)[56]. Another small hydrophilic analyte, lactate, is charged and therefore undergoes paracellular transport and filtration. Blood correlation of sweat lactate is confounded because it is also produced locally during sweat generation by glycogen breakdown in the clear cells lining the secretory coil[64].

Unlike glucose and lactate, small lipophilic (hydrophobic) molecules such as cortisol (one to tens of nanomolar) exhibit strong correlation between sweat and blood plasma concentrations[11,65], likely because they readily partition transcellularly through the lipophilic cell membranes[39]. This is expected to be true for other steroid hormones (progesterone, testosterone, etc.). Importantly, though, blood plasma correlation should only be expected for unbound (active) fractions in blood plasma; for example, cortisol bound to a large protein will partition no more easily than the very large protein itself. Like cortisol, many legal and illicit drugs are likely to correlate between sweat and blood plasma, as many are also small and lipophilic (for example, diamorphine, codeine and fentanyl), but larger or hydrophilic drugs are likely to be diluted (for example, penicillin, ibuprofen or amoxicillin).

Sweat does not have the gingival partitioning path of saliva, and sweat protein content is dominated by those proteins that are actively secreted (for example, dermicidin at 9.4–41.7 μM[11,51]) but also contains passively transported proteins, typically at >1,000-fold lower concentrations than ISF and blood plasma (one to tens of picomolar). For larger hydrophilic molecules and proteins, the paracellular partitioning pathway is not yet fully understood, but it has been speculated that proteins that are too large to pass through by filtering instead enter by a tight-junction remodeling effect[56,66]. As the tight junctions (Fig. 2a) remodel themselves[67], those adjacent to the lumen of the sweat gland will release their contents, which originated from ISF. If this speculated partitioning route is accurate, it could explain why proteins, such as cytokines, although highly dilute, are still found in sweat at their corresponding blood plasma ratios, regardless of their differing structures and molecular weights[68,69]. It should therefore not be surprising that even larger analytes, such as viral antibodies, are detectable in sweat[62]. This dilution of large analytes may actually have one benefit from a biosensing perspective: proteases and enzymes are therefore also highly dilute and will much more slowly break down or metabolize their analyte targets.

Sampling technology and devices. Sweat sampling can be divided into two general categories: positive-pressure-driven flow into microfluidic collectors and devices, or negative-pressure, wicking-driven flow into hydrophilic channels and wicking materials. A major challenge is sample volume. For example, at 1 nL min^{-1} per gland and an active gland density of 100 glands cm^{-2}, it would require 100 min to create a layer of sweat that is 100 μm thick (1 min for every micrometer of thickness). This immediately shows that a standard wicking textile, paper or microfluidic channel could face a serious challenge in providing sweat for fast sampling. If a positive pressure system is used, oil can be used to mitigate this dead volume and also reduce analyte contamination coming from the stratum corneum[70]. Similarly, and simpler to implement, a negative pressure system using an open microfluidic wick (Fig. 5e) can void the skin surface of sweat and do so with an effective wicking thickness of only ~1 μm, resulting in mere minutes from time of sweat secretion to sensing[71].

A variety of optical and electrical sensing modalities are possible, resulting in fully integrated devices ranging from the sizes of tattoos to Band-Aid like patches, to bands or straps[1,51], including fully integrated sweat stimulation[11,53]. Unfortunately, nearly all continuous sweat biosensing device demonstrations have not included sufficient blood plasma correlation data to confirm their potential impact, with only one recent article showing continuous sweat–blood correlated data for ethanol[59]. For most applications outside of active perspirers (athletes, workers), artificial sweat stimulation is required; otherwise, lack of dependable access makes sweat an inferior biofluid to saliva or tears. Localized sweat stimulation (Fig. 6) has been achieved for time scales ranging from hours to days by iontophoretic delivery of an electrically charged cholinergic agent, such as pilocarpine or carbachol[11,52].

Challenges and outlook. Perhaps the biggest inherent challenge for sweat biosensing is to correct for confounding factors caused by diluted (filtered) analyte partitioning. For dilution, this can be partially addressed by carefully stimulating sweat at a controlled secretion rate and/or by carefully measuring sweat generation rate and correcting for dilution. In some cases, it may be preferable to measure analyte ratios (for example, if the analyte of interest is a protein with a similar size to albumin, albumin could be used as a reference, as its blood plasma concentrations are stable). Sensor implementation must be carefully considered, and sensor results in a beaker are not necessarily applicable to such small sample volumes and a continuous flow of sample. For example, enzymatic sensors can be flow rate dependent[59]; this may represent a major technological oversight that may have given false promise to sweat sensing of lactate[72]. Now that >24-h sweat stimulation[52,53] and effective sampling[70,71] have been demonstrated, the biggest remaining technological challenge is sensors. All demonstrations to date of continuous sensing[51] have been for micromolar electrolytes (ion-selective electrodes) and micromolar metabolites (enzymatic sensors). Beyond those sensors, there is only one proven class of sensors for micromolar to nanomolar detection based on electrochemical aptamers[26], with none yet demonstrated for sweat. Additional technological advances may be required for analytes diluted nanomolar to picomolar, such as preconcentration[73] and chelation (tight junction release)[56].

Conclusions and perspective

ISF has a substantial advantage over other biofluids in terms of molecular weight cutoff and maximum dilution because it has very little dilution and, for most analytes, has a correlation with blood plasma concentration of nearly 1:1. For noninvasive approaches (i.e., saliva, sweat and tears), sweat may have the strongest advantage in maximizing blood plasma correlation because it can be stimulated to a steady secretion rate and because its secretion rate can be accurately measured using microfluidic flow meters. However, without knowing the secretion rate for saliva and tears, analyte ratios could instead be measured (for example, one could measure the ratio

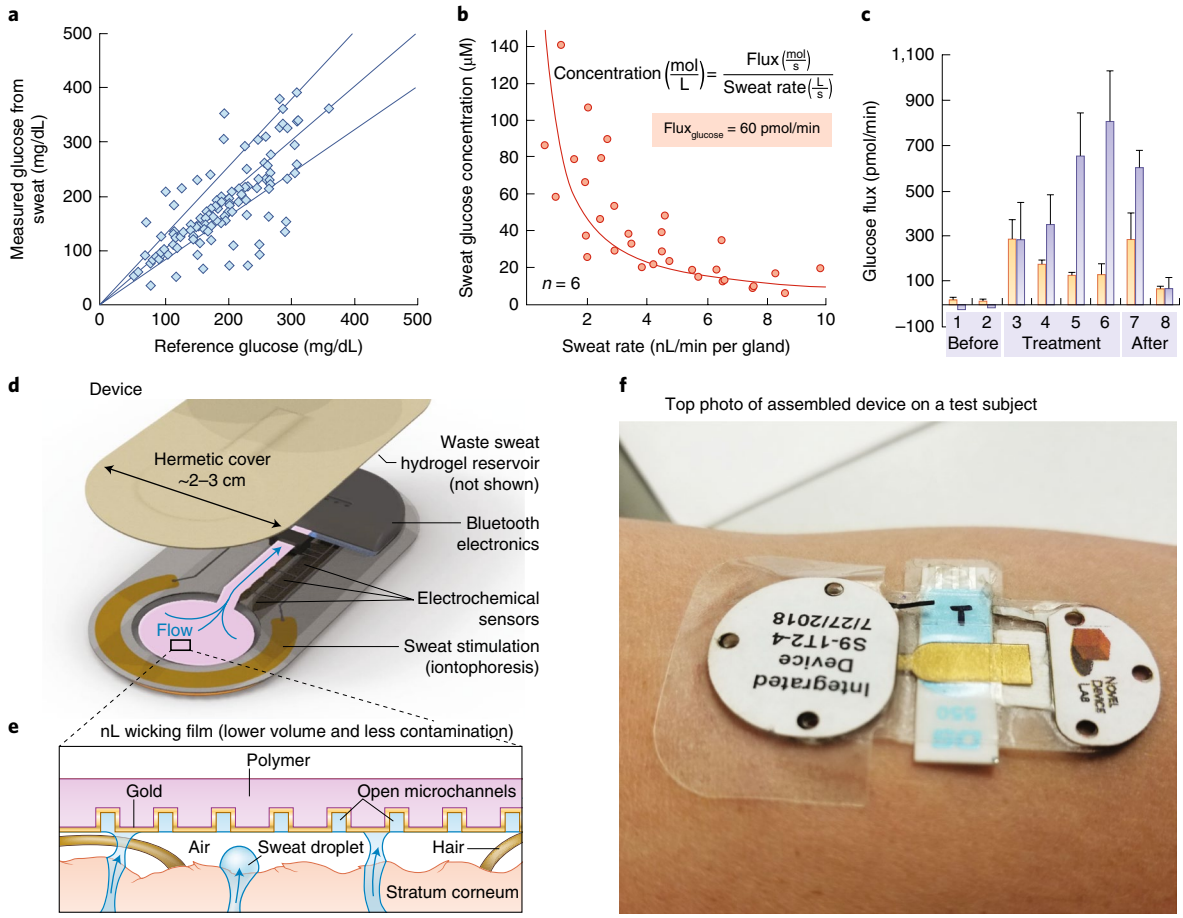


Fig. 5 | Sweat data for glucose. a, Predicted (measured) blood glucose values from sweat glucose versus a corresponding reference blood glucose value[63] collected at uncontrolled sweat rates. The upper and lower lines represent +20% and -20%, respectively, about the linear fit (middle line). **b**, Dilution of glucose versus increasing sweat generation from 6 different subjects[56]. **c**, Enhancement of paracellular glucose flux by treatment with reverse iontophoresis (gold bars) and by treatment with reverse iontophoresis and tight junction modulation by chelation (blue bars)[56]. The data are plotted chronologically (1, 2 are baseline; 3, 4, 5, 6 are treatments; 7, 8 are post-baseline; each corresponds to a 20-min sample collection period) with s.e.m. error bars. **d**, Diagram of a proposed wearable sweat biosensing device. **e**, Diagram of an in vivo validated wicking material for minimizing sample volumes and reducing contamination from the stratum corneum[71]. **f**, Example photos of an integrated device with all components, except the wireless electronics and battery (credit: Adam Hauke and Philip Simmers, Univ. Cincinnati[59]).

between a cytokine and albumin, which has a steady blood plasma concentration). Advective transport affects system complexity and is likely needed for sweat sensing to quickly pull tiny volumes of sweat off the skin surface and move it to a sensor[59,71]. Advective transport does bring potential advantages, however, as it can enable simple preconcentration techniques that can help mitigate analyte dilution[73]. Sample production rate is a challenge for both sweat and tears, requiring challenging miniaturization of transport and sensing components. However, ISF sampling also requires challenging miniaturization, as the goal is to make the smallest possible holes through the skin.

Maximum temporal resolution (lag time) is a potential advantage for sweat because sweat is directionally secreted and the glands are highly vascularized. However, a short lag time is only needed for a small subset of analytes (for example, glucose in diabetes, lactate threshold in athletics, or cortisol awakening response). The lag time values shown in Table 1 assume high-quality sample collection (such as no mixing of new and old samples of biofluid). Sweat and ISF have advantages in controllable secretion rates, which are important for diluted analytes, the concentration of which can vary widely as secretion rate changes. However, for sweat, chemical stimulation will be required[52,53,59] for many applications and could complicate device design. Research maturity has come a long way for ISF, saliva and more recently sweat, and numerous technological solutions have been demonstrated to deal with potential confounding issues. Only ISF and saliva have substantial commercial maturity, with tears having no current biochemical sensing products and sweat having only one current product, used for cystic fibrosis testing[54].

ISF has enjoyed steady forward momentum in all categories that matter: ergonomics, lag time, sensor accuracy and sensor stability. But progress for this biofluid has been mainly limited to glucose sensing for diabetes care. It is worth pointing out that patients with diabetes endure considerable discomfort (blood pricks, implanted needles, etc.) because their daily survival depends on it. For the third wave of devices to expand to users who have less acute needs, many devices will likely need to be less invasive and easier to use.

Momentum for saliva has been quite different from that for ISF, as saliva does not have a single dominant use and has seen most of its growth in pursuit of different analytes for single-use tests. No continuous saliva-testing products currently exist, likely, in some cases, because wearability is an issue (for example, a mouth guard is undesirable for many; Fig. 4e).

Recently, many technological advances have been made in sweat biosensing, especially in integrated and prolonged stimulation, without which users are limited to active perspirers such as athletes

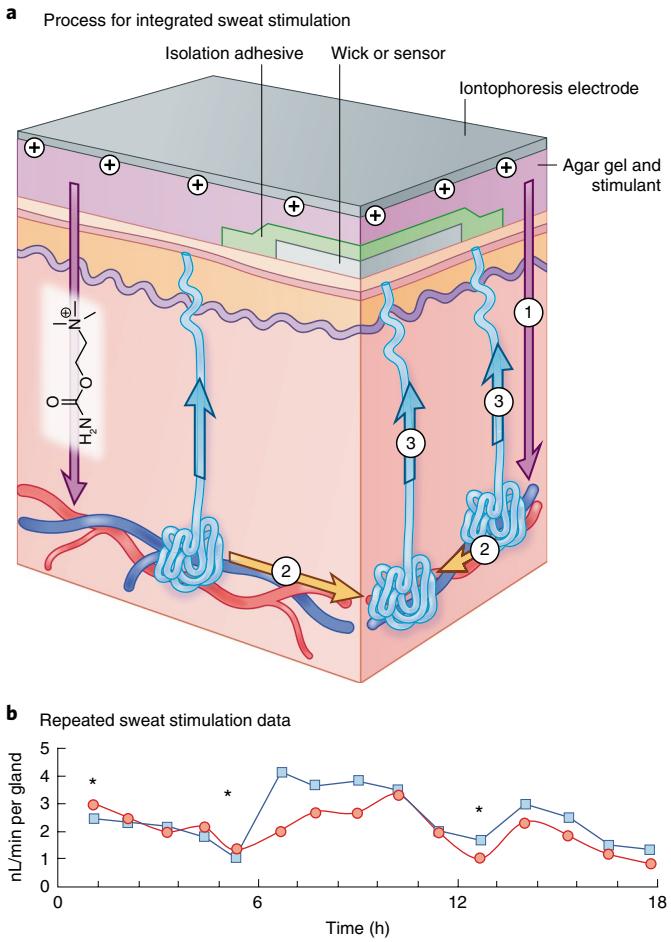


Fig. 6 | Sweat stimulation approaches. a, Integrated iontophoretic sweat stimulation[53] without cross-contamination between the stimulant gel and the wicking material and/or sensor. Preventing this cross-contamination requires adhesive isolation or other forms of isolation, and the following: (1) iontophoretic delivery of a cholinergic agent such as carbachol, (2) cross-delivery of the stimulant and/or sudomotor axon cross-coupling of the stimulation response, and (3) stimulated sweat generation even in areas not directly underneath the stimulant gel. **b**, Stimulation can also be repeated (asterisks) to sustain a sweat generation response of >1 nL min^{-1} per gland (two tests for one subject are shown)[52].

or industrial workers. Continuous sensing with ISF and sweat are poised to gain the most advantage from device miniaturization because for saliva too much miniaturization could result in a greater risk of the user swallowing the detection device.

The use of tears, whether for one-time tests or for continuous sensing, is not competitive with saliva or sweat. It may be that for quick one-time tests saliva and blood will be primary competitors and for continuous sensing ISF and sweat will be primary competitors. For sweat, device architecture (Fig. 5) could require more device components than that for ISF, as ISF testing simply embeds a needle and sensor in the fluid (Fig. 3). Furthermore, the total number of analytes in sweat that can be correlated with blood plasma is certainly fewer than for ISF. However, because sweat sensing does not require implantable devices, it might be able to exploit shorter-lasting sensors, preconcentration[73] and other technologies that are more feasible ex vivo. For example, making an indwelling and long-lasting sensor for the protein IL-6 in ISF is likely more difficult than preconcentrating IL-6 in sweat and measuring it with an array of short-lasting sensors.

Because saliva and blood are needed mostly for one-time tests, sensor development for these fluids is much easier, given that lateral flow assays and other conventional assays can exploit the very low detection limits of antibodies. Wearable devices for ISF, saliva, sweat and tears all share a potential competitor in sensors implanted in the body, although this last faces considerable technical challenges, such as sensor longevity. Both for wearables and for implanted sensors, the greatest need is for robust, continuous sensors in all biofluids, and this goal deserves particular attention from researchers.

Human subjects

Aspects of this study were performed under University of Cincinnati IRB protocol study 2016-4769. The glucose flux experiment consisted of 6 healthy participants (5 male, 1 female) between approximately 20 and 40 years old.

Received: 9 March 2018; Accepted: 20 November 2018;
Published online: 25 February 2019

References

1. Heikenfeld, J. et al. Wearable sensors: modalities, challenges, and prospects. *Lab Chip* **18**, 217–248 (2018).
2. Allied Analytics LLP. *Continuous Glucose Monitoring Systems Market by Components, Demographics, and Adult Population, and End User – Global Opportunity Analysis and Industry Forecast, 2016–2024* (Allied Analytics, 2018).
3. Engler, R., Routh, T. L. & Lucisano, J. Y. Adoption barriers for continuous glucose monitoring and their potential reduction with a fully implanted system: results from patient preference surveys. *Clin. Diabetes* **36**, 50–58 (2018).
4. Christiansen, M. P. et al. A prospective multicenter evaluation of the accuracy of a novel implanted continuous glucose sensor: PRECISE II. *Diabetes Technol. Ther.* **20**, 197–206 (2018).
5. Farandos, N. M., Yetisen, A. K., Monteiro, M. J., Lowe, C. R. & Yun, S. H. Contact lens sensors in ocular diagnostics. *Adv. Healthc. Mater.* **4**, 792–810 (2015).
6. Anderson, J. M. & Van Itallie, C. M. Physiology and function of the tight junction. *Cold Spring Harb. Perspect. Biol.* **1**, a002584 (2009).
7. Rana, R., Minhas, L.A. & Mubarik, A. Histological study of human sublingual gland with special emphasis on intercalated and striated ducts. *Pak. Armed Forces Med. J.* **62**, 606–611 (2012).
8. Zenk, J., Hosemann, W. G. & Iro, H. Diameters of the main excretory ducts of the adult human submandibular and parotid gland: a histologic study. *Oral Surg. Oral Med. Oral Pathol. Oral Radiol. Endod.* **85**, 576–580 (1998).
9. Hellquist, H. & Skalova, A. Histology. in *Histopathology of the Salivary Glands* 1–22, https://doi.org/10.1007/978-3-540-46915-5_1 (Springer, Berlin and Heidelberg, Germany, 2014).
10. Boysen, T. C., Yanagawa, S., Sato, F. & Sato, K. A modified anaerobic method of sweat collection. *J. Appl. Physiol.* **56**, 1302–1307 (1984).
11. Sonner, Z. et al. The microfluidics of the eccrine sweat gland, including biomarker partitioning, transport, and biosensing implications. *Biomicrofluidics* **9**, 031301 (2015).
12. Guyton, A. C. A concept of negative interstitial pressure based on pressures in implanted perforated capsules. *Circ. Res.* **12**, 399–414 (1963).
13. Fogh-Andersen, N., Altura, B. M., Altura, B. T. & Siggaard-Andersen, O. Composition of interstitial fluid. *Clin. Chem.* **41**, 1522–1525 (1995).
14. Cohen, J. et al. Measurement of tissue cortisol levels in patients with severe burns: a preliminary investigation. *Crit. Care* **13**, R189 (2009).
15. Cooke, I. M., Bevill, R. P., Nelson, D. R. & Koritz, G. D. Pharmacokinetics of penicillin G in plasma and interstitial fluid collected with dialysis fiber bundles in sheep. *Vet. Res.* **27**, 147–159 (1996).
16. Zeitlinger, M. A. et al. Protein binding: do we ever learn? *Antimicrob. Agents Chemother.* **55**, 3067–3074 (2011).
17. Gottås, A. et al. Levels of heroin and its metabolites in blood and brain extracellular fluid after i.v. heroin administration to freely moving rats. *Br. J. Pharmacol.* **170**, 546–556 (2013).
18. Vermeer, B. J., Reman, F. C. & van Gent, C. M. The determination of lipids and proteins in suction blister fluid. *J. Invest. Dermatol.* **73**, 303–305 (1979).
19. Bailey, T., Bode, B. W., Christiansen, M. P., Klaff, L. J. & Alva, S. The performance and usability of a factory-calibrated flash glucose monitoring system. *Diabetes Technol. Ther.* **17**, 787–794 (2015).
20. Jina, A. et al. Design, development, and evaluation of a novel microneedle array-based continuous glucose monitor. *J. Diabetes Sci. Technol.* **8**, 483–487 (2014).

21. Cunningham, D.D. Transdermal microfluidic continuous monitoring systems. in *In Vivo Glucose Sensing* 191–215, https://doi.org/10.1002/9780470567319.ch7 (Wiley, 2010).
22. Miller, P. R. et al. Extraction and biomolecular analysis of dermal interstitial fluid collected with hollow microneedles. *Commun. Biol.* **1**, 173 (2018).
23. Ripolin, A. et al. Successful application of large microneedle patches by human volunteers. *Int. J. Pharm.* **521**, 92–101 (2017).
24. Lewis, D. R. & Chadha, J. S. AlphaWise diabetes survey: ABT's Libre underappreciated; MDT acceleration likely; price the concern for DXCM. Morgan Stanley Research 1–24 (2018).
25. Hoss, U., Budiman, E. S., Liu, H. & Christiansen, M. P. Feasibility of factory calibration for subcutaneous glucose sensors in subjects with diabetes. *J. Diabetes Sci. Technol.* **8**, 89–94 (2014).
26. Arroyo-Currás, N. et al. Real-time measurement of small molecules directly in awake, ambulatory animals. *Proc. Natl. Acad. Sci. USA* **114**, 645–650 (2017).
27. Humphrey, S. P. & Williamson, R. T. A review of saliva: normal composition, flow, and function. *J. Prosthet. Dent.* **85**, 162–169 (2001).
28. Wong, D. T. Towards a simple, saliva-based test for the detection of oral cancer. *Expert Rev. Mol. Diagn.* **6**, 267–272 (2006).
29. Ship, J. A. & Fischer, D. J. The relationship between dehydration and parotid salivary gland function in young and older healthy adults. *J. Gerontol. A Biol. Sci. Med. Sci.* **52**, M310–M319 (1997).
30. Proctor, G. B. & Carpenter, G. H. Regulation of salivary gland function by autonomic nerves. *Auton. Neurosci.* **133**, 3–18 (2007).
31. Veerman, E. C. I., van den Keybus, P. A., Vissink, A. & Nieuw Amerongen, A. V. Human glandular salivas: their separate collection and analysis. *Eur. J. Oral Sci.* **104**, 346–352 (1996).
32. Proctor, G. B. The physiology of salivary secretion. *Periodontol. 2000* **70**, 11–25 (2016).
33. Villiger, M. et al. Evaluation and review of body fluids saliva, sweat and tear compared to biochemical hydration assessment markers within blood and urine. *Eur. J. Clin. Nutr.* **72**, 69–76 (2018).
34. Makaram, P., Owens, D. & Aceros, J. Trends in nanomaterial-based non-invasive diabetes sensing technologies. *Diagnostics (Basel)* 4, (27–46 (2014).
35. Vasconcelos, A. C. U., Soares, M. S. M., Almeida, P. C. & Soares, T. C. Comparative study of the concentration of salivary and blood glucose in type 2 diabetic patients. *J. Oral Sci.* **52**, 293–298 (2010).
36. Segura, R. et al. A new approach to the assessment of anaerobic metabolism: measurement of lactate in saliva. *Br. J. Sports Med.* **30**, 305–309 (1996).
37. Oliveira, L. D. S., Oliveira, S. F., Manchado-Gobatto, F. D. B. & Costa, M. D. C. Salivary and blood lactate kinetics in response to maximal workload on cycle ergometer. *Revista Brasileira de Cineantropometria & Desempenho Humano* **17**, 565 (2015).
38. Kiang, T. K. L. & Ensom, M. H. H. A qualitative review on the pharmacokinetics of antibiotics in saliva: implications on clinical pharmacokinetic monitoring in humans. *Clin. Pharmacokinet.* **55**, 313–358 (2016).
39. Vining, R. F. & McGinley, R. A. The measurement of hormones in saliva: possibilities and pitfalls. *J. Steroid Biochem.* **27**, 81–94 (1987).
40. Jaedicke, K. M., Preshaw, P. M. & Taylor, J. J. Salivary cytokines as biomarkers of periodontal diseases. *Periodontol. 2000* **70**, 164–183 (2016).
41. Korte, D. L. & Kinney, J. Personalized medicine: an update of salivary biomarkers for periodontal diseases. *Periodontol. 2000* **70**, 26–37 (2016).
42. Sapna, G., Gokul, S. & Bagri-Manjrekar, K. Matrix metalloproteinases and periodontal diseases. *Oral Dis.* **20**, 538–550 (2014).
43. Slavish, D. C., Graham-Engeland, J. E., Smyth, J. M. & Engeland, C. G. Salivary markers of inflammation in response to acute stress. *Brain Behav. Immun.* **44**, 253–269 (2015).
44. Myette-Côté, É., Baba, K., Brar, R. & Little, J. P. Detection of salivary insulin following low versus high carbohydrate meals in humans. *Nutrients* **9**, 1204 (2017).
45. Branson, B. M. FDA approves OraQuick for use in saliva. *AIDS Clin. Care* **16**, 39 (2004).
46. Foudeh, A. M., Fatanat Didar, T., Veres, T. & Tabrizian, M. Microfluidic designs and techniques using lab-on-a-chip devices for pathogen detection for point-of-care diagnostics. *Lab Chip* **12**, 3249–3266 (2012).
47. Parry, J. V., Perry, K. R. & Mortimer, P. P. Sensitive assays for viral antibodies in saliva: an alternative to tests on serum. *Lancet* **2**, 72–75 (1987).
48. Granger, D. A. et al. Focus on methodology: salivary bioscience and research on adolescence: an integrated perspective. *J. Adolesc.* **35**, 1081–1095 (2012).
49. Kim, J. et al. Wearable salivary uric acid mouthguard biosensor with integrated wireless electronics. *Biosens. Bioelectron.* **74**, 1061–1068 (2015).
50. Ritzer, J. et al. Diagnosing peri-implant disease using the tongue as a 24/7 detector. *Nat. Commun.* **8**, 264 (2017).
51. Heikenfeld, J. Non-invasive analyte access and sensing through eccrine sweat: challenges and outlook circa 2016. *Electroanalysis* **28**, 1242–1249 (2016).
52. Simmers, P., Li, S. K., Kasting, G. & Heikenfeld, J. Prolonged and localized sweat stimulation by iontophoretic delivery of the slowly-metabolized cholinergic agent carbachol. *J. Dermatol. Sci.* **89**, 40–51 (2018).
53. Sonner, Z., Wilder, E., Gaillard, T., Kasting, G. & Heikenfeld, J. Integrated sudomotor axon reflex sweat stimulation for continuous sweat analyte analysis with individuals at rest. *Lab Chip* **17**, 2550–2560 (2017).
54. Desax, M.-C., Ammann, R. A., Hammer, J., Schoeni, M. H. & Barben, J. Nanoduct sweat testing for rapid diagnosis in newborns, infants and children with cystic fibrosis. *Eur. J. Pediatr.* **167**, 299–304 (2008).
55. Bourne, G. H. & Danielli, J. F. *International Review of Cytology* Vol. 87 (Academic, 1984).
56. Jajack, A., Brothers, M., Kasting, G. & Heikenfeld, J. Enhancing glucose flux into sweat by increasing paracellular permeability of the sweat gland. *PLoS One* **13**, e0200009 (2018).
57. Bovell, D. The human eccrine sweat gland: structure, function and disorders. *J. Local Glob. Health Sci.* **2015**, 5 (2015).
58. Hurley, H. J. & Witkowski, J. Dye clearance and eccrine sweat secretion in human skin. *J. Invest. Dermatol.* **36**, 259–272 (1961).
59. Hauke, A. et al. Complete validation of a continuous and blood-correlated sweat biosensing device with integrated sweat stimulation. *Lab Chip* **18**, 3750–3759 (2018).
60. Choi, J. et al. Soft, skin-mounted microfluidic systems for measuring secretory fluidic pressures generated at the surface of the skin by eccrine sweat glands. *Lab Chip* **17**, 2572–2580 (2017).
61. Baker, L. B. Sweating rate and sweat sodium concentration in athletes: a review of methodology and intra/interindividual variability. *Sports Med.* **47** (Suppl. 1), 111–128 (2017).
62. Katchman, B., Zhu, M., Cristen, J. B. & Anderson, K. S. Eccrine sweat as a biofluid for profiling immune biomarkers. *Proteomics Clin. Appl.* **12**, e1800010 (2018).
63. Moyer, J., Wilson, D., Finkelshtein, I., Wong, B. & Potts, R. Correlation between sweat glucose and blood glucose in subjects with diabetes. *Diabetes Technol. Ther.* **14**, 398–402 (2012).
64. Ament, W., Huizenga, J. R., Mook, G. A., Gips, C. H. & Verkerke, G. J. Lactate and ammonia concentration in blood and sweat during incremental cycle ergometer exercise. *Int. J. Sports Med.* **18**, 35–39 (1997).
65. Jia, M., Chew, W. M., Feinstein, Y., Skeath, P. & Sternberg, E. M. Quantification of cortisol in human eccrine sweat by liquid chromatography – tandem mass spectrometry. *Analyst* **141**, 2053–2060 (2016).
66. La Count, T. D., Jajack, A., Heikenfeld, J. & Kasting, G. B. Modeling glucose transport from systemic circulation to sweat. *J. Pharm. Sci.* **108**, 364–371 (2019).
67. Steed, E., Balda, M. S. & Matter, K. Dynamics and functions of tight junctions. *Trends Cell Biol.* **20**, 142–149 (2010).
68. Marques-Deak, A. et al. Measurement of cytokines in sweat patches and plasma in healthy women: validation in a controlled study. *J. Immunol. Methods* **315**, 99–109 (2006).
69. Cizza, G. et al. Elevated neuroimmune biomarkers in sweat patches and plasma of premenopausal women with major depressive disorder in remission: the POWER study. *Biol. Psychiatry* **64**, 907–911 (2008).
70. Peng, R. et al. A new oil/membrane approach for integrated sweat sampling and sensing: sample volumes reduced from µL's to nL's and reduction of analyte contamination from skin. *Lab Chip* **16**, 4415–4423 (2016).
71. Twine, N. B. et al. Open nanofluidic films with rapid transport and no analyte exchange for ultra-low sample volumes. *Lab Chip* **18**, 2816–2825 (2018).
72. Jia, W. et al. Electrochemical tattoo biosensors for real-time noninvasive lactate monitoring in human perspiration. *Anal. Chem.* **85**, 6553–6560 (2013).
73. Jajack, A. et al. Continuous, quantifiable, and simple osmotic preconcentration and sensing within microfluidic devices. *PLoS One* **14**, e0210286 (2019).
74. OpenStax. Epithelial tissue. *OpenStax CNX* http://cnx.org/contents/a16a9513-1ac9-495d-9096-bb8b31905a44@3 (2016).
75. Kim, Y. C., Park, J. H. & Prausnitz, M. R. Microneedles for drug and vaccine delivery. *Adv. Drug Deliv. Rev.* **64**, 1547–1568 (2012).
76. Zhang, W., Du, Y. & Wang, M. L. On-chip highly sensitive saliva glucose sensing using multilayer films composed of single-walled carbon nanotubes, gold nanoparticles, and glucose oxidase. *Sens. Biosensing Res.* **4**, 96–102 (2015).
77. Perogamvros, I., Keevil, B. G., Ray, D. W. & Trainer, P. J. Salivary cortisone is a potential biomarker for serum free cortisol. *J. Clin. Endocrinol. Metab.* **95**, 4951–4958 (2010).
78. Fullard, R. J. & Snyder, C. Protein levels in nonstimulated and stimulated tears of normal human subjects. *Invest. Ophthalmol. Vis. Sci.* **31**, 1119–1126 (1990).
79. Runström, G., Mann, A. & Tighe, B. The fall and rise of tear albumin levels: a multifactorial phenomenon. *Ocul. Surf.* **11**, 165–180 (2013).
80. Sørensen, T. & Jensen, F. T. Tear flow in normal human eyes. Determination by means of radioisotope and gamma camera. *Acta Ophthalmol. (Copenh.)* **57**, 564–581 (1979).
81. Mishima, S., Gasset, A., Klyce, S. D. Jr. & Baum, J. L. Determination of tear volume and tear flow. *Invest. Ophthalmol.* **5**, 264–276 (1966).

82. Kallapur, B. et al. Quantitative estimation of sodium, potassium and total protein in saliva of diabetic smokers and nonsmokers: a novel study. *J. Nat. Sci. Biol. Med.* **4**, 341–345 (2013).
83. Brandtzaeg, P. Do salivary antibodies reliably reflect both mucosal and systemic immunity? *Ann. NY Acad. Sci.* **1098**, 288–311 (2007).
84. Vairo, D. et al. Towards addressing the body electrolyte environment via sweat analysis: pilocarpine iontophoresis supports assessment of plasma potassium concentration. *Sci. Rep.* **7**, 11801 (2017).
85. Green, J. M., Bishop, P. A., Muir, I. H., McLester, J. R. Jr. & Heath, H. E. Effects of high and low blood lactate concentrations on sweat lactate response. *Int. J. Sports Med.* **21**, 556–560 (2000).
86. Derbyshire, P. J., Barr, H., Davis, F. & Higson, S. P. J. Lactate in human sweat: a critical review of research to the present day. *J. Physiol. Sci.* **62**, 429–440 (2012).
87. Bruen, D., Delaney, C., Florea, L. & Diamond, D. Glucose sensing for diabetes monitoring: recent developments. *Sensors (Basel)* 17, (1866 (2017).
88. Jung, K. et al. The sweat of patients with atopic dermatitis contains specific IgE antibodies to inhalant allergens. *Clin. Exp. Dermatol.* **21**, 347–350 (1996).

Acknowledgements

Authors at the University of Cincinnati and Eccrine Systems would like to acknowledge support from the Air Force Research Labs (USAF contract #FA8650-16-C-6760). The University of Cincinnati authors further acknowledge support from the National Science Foundation (EPMD award #ECCS-1608275), the Ohio Federal Research Network (PO FY16-049; WSARC-1077-700), Eccrine Systems and the industrial members of the Center for Advanced Design and Manufacturing of Integrated Microfluidics (NSF I/UCRC award #IIP-1738617).

Author contributions

J.H. led the organization and revision of the manuscript, and all other others contributed to the writing. A.J led the local structure section; B.F. the ISF section; S. Granger and S. Gaitonde the saliva section; J.H., G.B. and B.K. the sweat section; and J.H. the introduction and discussion sections.

Competing interests

J.H. is the Chief Science Officer and cofounder of Eccrine Systems, Inc., which is commercializing sweat biosensing technology. B.F. is an employee of Abbott Diabetes Care, which produces and markets the FreeStyle Libre Flash Glucose Monitoring System. S. Granger and S. Gaitonde are employees of Salimetrics LLC, which commercializes saliva biosensing devices.

Additional information

Reprints and permissions information is available at www.nature.com/reprints.

Correspondence should be addressed to A.J.

Publisher's note: Springer Nature remains neutral with regard to jurisdictional claims in published maps and institutional affiliations.

© Springer Nature America, Inc. 2019